ACS APPLIED MATERIALS & INTERFACES

Research Article

www.acsami.org

UV-Curable Nanocomposite Based on Methacrylic-Siloxane Resin and Surface-Modified TiO_2 Nanocrystals

Chiara Ingrosso,[†] Carola Esposito Corcione,[‡] Raffaella Striani,[‡] Roberto Comparelli,[†] Marinella Striccoli,[†] Angela Agostiano,[†,§] M. Lucia Curri,*[,†] and Mariaenrica Frigione[‡]

[†]CNR-IPCF U.O.S. Bari, c/o Department of Chemistry, University of Bari, Via Orabona, 70126 Bari, Italy

[‡]Department of Engineering for Innovation, University of Salento, Via Arnesano, I-73100 Lecce, Italy

[§]Department of Chemistry, University of Bari, Via Orabona 4, I-70126 Bari, Italy

Supporting Information

ABSTRACT: A novel UV-light-curable nanocomposite material formed of a methacrylic-siloxane resin loaded with 1 wt % oleic acid and 3-(trimethoxysilyl)propyl methacrylate silane (OLEA/MEMO)-coated TiO_2 nanorods (NRs) has been manufactured as a potential self-curing structural coating material for protection of monuments and artworks, optical elements, and dental components. OLEA-coated TiO_2 NRs, presynthesized by a colloidal chemistry route, have been surface-modified by a treatment with the methacrylic-based silane coupling agent MEMO. The resulting OLEA/MEMO-capped TiO_2 NRs have been dispersed in MEMO; that is a monomer precursor of the organic formulation, used as a "common solvent" for transferring the NRs in prepolymer components of the formulation. Differential scanning calorimetry and Fourier transform infrared spectroscopy have allowed investigation of the effects of the incorporation of the OLEA/MEMO-capped TiO_2 NRs on reactivity and photopolymerization kinetics of the nanocomposite, demonstrating that the embedded NRs significantly increase curing reactivity of the neat organic formulation both in air and inert atmosphere. Such a result has been explained on the basis of the photoactivity of the nanocrystalline TiO_2 which behaves as a free-radical donor photocatalyst in the curing reaction, finally turning out more effective than the commonly used commercial photoinitiator. Namely, the NRs have been found to accelerate the cure rate and increase cross-linking density, promoting multiple covalent bonds between the resin prepolymers and the NR ligand molecules, and, moreover, they limit inhibition effect of oxygen on photopolymerization. The NRs distribute uniformly in the photocurable matrix, as assessed by transmission electron microscopy analysis, and increase glass transition temperature and water contact angle of the nanocomposite with respect to the neat resin.

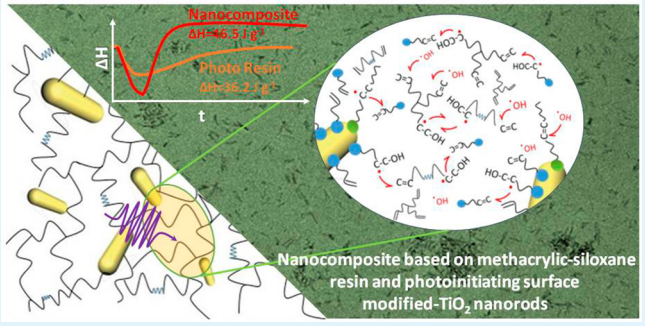

KEYWORDS: *colloidal TiO_2 nanorods, surface modification, photoactivity, UV-curable methacrylic−siloxane resin formulation, nanocomposite, photopolymerization kinetic*

1. INTRODUCTION

Nanocomposite materials have recently attracted the attention of the scientific community for their interesting functionalities, arising from synergic combination of unique size- and shape-dependent properties of inorganic nanofillers (i.e., electrical, magnetic, catalytic, and optical) and those outstanding of host polymers (i.e., mechanical flexibility, low weight, and prompt processability). Such multifunctional materials can be successfully used in high-added-value applications for fabricating components of catalysts, sensors, lenses, electronics, mechanics, dental fillings, molds, inks, protective coatings, packages, adhesives, and varnishes.[1−4]

Incorporation of inorganic nanoparticles (NPs) in an organic host matrix suffers, however, for the tendency of nanofillers to aggregate and consequently to poorly disperse in the polymer matrix, thus being detrimental for the final functionalities of the nanocomposite. NPs and, in particular, colloidal nanocrystals (NCs) are ideal nanofillers for manufacturing highly promising functional nanocomposites.[5,6] The organic molecules coordinating NC surface impart them with a surface chemistry that can be tuned, by designing and implementing suitable ligand exchange procedures.[7] Such a strategy improves compatibility and stabilization of NCs in an organic host, resulting in a high interface area between the two components, and grants transfer of intrinsic size- and shape-dependent functionalities of NCs to the nanocomposite, preserving, at the same time, processability of the organic formulation.[5,6]

Here, organic-coated rod-shaped TiO_2 NCs, anatase in phase, have been incorporated in a UV-light-curable methacrylic-siloxane resin formulation, recently optimized by the

Received: May 3, 2015
Accepted: June 25, 2015
Published: July 7, 2015

DOI: 10.1021/acsami.5b03731
ACS Appl. Mater. Interfaces 2015, 7, 15494−15505

authors,[8,9] which is based on both methacrylic and siloxane monomers, namely, trimethylolpropane trimethacrylate (TMPTMA), 3-(trimethoxysilyl)propyl methacrylate (MEMO), and a vinyl-terminated polydimethylsiloxane (VT PDMS), that are UV-light-photoinitiated by Irgacure819.

Curable formulations based on siloxane and methacrylic or acrylic monomers are characterized by adhesion on surfaces, hydrophobicity, optical transparency, capability to prevent infiltration of contaminants or degrading agents, permeability to water vapor, chemical compatibility with different inorganic substrates, and excellent antifouling and weathering resistance.[10,11] The low molecular weight of the monomers, the low viscosity of the formulation, and the in situ polymerization mechanism allow the resin penetration inside porous substrates, leading to a uniform and very adherent coating.[10,11] Such properties make them optimal materials for manufacturing water repellent and optically clear coatings for protection and conservation of stones and concrete buildings, lenses, dental elements and adhesives, and multifunctional finishing agents for textiles and leather components.[8,12,13]

The use of a UV-light photoinitiator for activating photopolymerization of formulations based on such monomers has been recently proposed as a valuable alternative to the thermally initiated curing[8,9] that is an approach typically used for preparing coatings for protection of natural stones. UV-light photoinitiation is a solvent-free curing mechanism based on a photopolymerization faster than that activated by a thermal initiator. Indeed, thermal curing requires up to several weeks to complete the reaction, and, hence, it is strongly affected by environmental conditions (i.e., temperature, humidity, and external contamination). The fast UV curing process results, especially in outdoor and large surface area applications, in highly adherent, stable, and, completely cured coatings, exhibiting a glass transition temperature (T_g) higher than those achieved by means of thermal polymerization or by solution processes, whose T_g anyway never exceeds 40 °C.[14]

Inorganic spherical semiconductor NPs, such as CdS, Fe_2O_3, ZnO, and TiO_2, have been investigated as free-radical photoinitiators for curing acrylic and methacrylic resins, due to their capability of generating, under photoexcitation, electron−hole pairs, which react with resin monomers providing reactive radicals.[15−17] For such systems, photopolymerization quantum yield decreases with particle size, because benefits arising from higher surface-to-volume ratio with the small size are significantly offset by the increase of electron−hole recombination at surface defect trapping sites.[18] However, the use of NPs as photoinitiators and, concomitantly, as functional nanofillers for conveying selected properties to the curable host matrix, exploitable for specific technological applications, has not been explored so far.

Nanocrystalline TiO_2 is a wide band gap semiconductor, considered extremely interesting as nanofiller due to its low toxicity, high refractive index, optical transparency in the visible spectral range, low cost, photostability and photoactivity under UV light, and mechanical strength. TiO_2 NPs have been incorporated in acrylic resins for manufacturing dental materials with antimicrobial activity[19] and visible transparent UV-shielding coatings,[20] in polyurethane polymers for fabricating antibacterial and self-cleaning coatings[21] and in epoxy resins for preparation of lenses, optical filters, waveguides, and antireflection films.[22]

Here, organic-coated highly crystalline TiO_2 NPs, synthesized by the colloidal route reported in ref 23 with a narrow size distribution in the most photoactive anatase phase[24] and in a rod shape, have been selected as functional and photoinitiating nanofillers of the UV-light-curable methacrylic-siloxane formulation. The elongated morphology of the NPs grants a lower recombination rate of the photogenerared electron−hole pairs, higher surface-to-volume ratio, and concomitantly higher density of active sites available for surface reactions, when compared to spherical NPs.[25]

The organic-capped TiO_2 NRs have demonstrated high processability, for the possibility to engineer their surface chemistry and impart them a suitable reactivity for the methacrylic-siloxane matrix. In particular, the presynthesized TiO_2 NRs have been made compatible with the methacrylic prepolymers of the curable matrix, by performing a ligand exchange procedure that partially removes the pristine hydrophobic oleic acid (OLEA) ligand molecules and grafts their surface with a methacrylic-based organofunctional silane coupling agent,[26] namely, 3-(trimethoxysilyl)propyl methacrylate (MEMO). The incorporation of the prepared OLEA/MEMO-coated TiO_2 NRs in MEMO, which is a resin prepolymer, used here as a "common solvent",[5,6] has been a preliminary step for their blending with the more viscous methacrylic and siloxane precursors of the resin formulation.

In addition, in formulating the UV-curable nanocomposite, possible damage due to the TiO_2 NR induced photocatalytic degradation of the host polymer matrix has been taken also into account. Indeed, since surface modification of TiO_2 NPs with a silica-based coating has been found to delay the -C−C- bond cleavage in sol−gel acrylic-based coatings,[27] OLEA/MEMO-capped TiO_2 NRs are expected to hamper photoactive degradation phenomena in the host matrix. Therefore, the formulation has been designed with a high content of the methacrylic-based silane MEMO and only a low amount of the other organic components. In addition, the NR loading has been kept rather low (1 wt %).

This work has aimed at investigating the effect of the incorporation of the functional nanofiller on reactivity and photopolymerization kinetics of the nanocomposite. A comprehensive structural, spectroscopic, and calorimetric investigation of the TiO_2 NR modified methacrylic-siloxane resin, performed by transmission electron microscopy, infrared spectroscopy, and (photo)differential scanning calorimetry, respectively, has assessed the uniform dispersion of the NRs in the host material and their self-curing ability.

To the best of our knowledge, the use of such a kind of rod-shaped colloidal nanocrystalline TiO_2 as photoinitiator has not been reported so far. Indeed, the careful kinetic study of the nanocomposite has demonstrated that the TiO_2 NRs effectively act as photoinitiator, ultimately controlling the curing process.

The achieved nanocomposite results in a relevant structural material with a large potential in technological applications for manufacturing self-curing coatings that concomitantly can show water repellence, self-cleaning, and UV-shielding properties for conservation of stones and concretes, dental elements, or optical components.

2. MATERIALS AND METHODS

2.1. Materials. All chemicals were at the highest purity available and used as received. Oleic acid (OLEA, 90%), titanium tetraisopropoxide ($Ti(O^iPr)_4$ or TTIP, 98.9%), and trimethylamino-*N*-oxide dihydrate ($(CH_3)_3NO{\cdot}2H_2O$ or TMAO, 98%) were purchased from Fluka. Trimethoxypropylsilane methacrylate (MEMO) was produced by Dow Corning, trimethylolpropane trimethacrylate (TMPTMA)

DOI: 10.1021/acsami.5b03731
ACS Appl. Mater. Interfaces 2015, 7, 15494−15505

was supplied by Cray Valley, bis(2,4,6-trimethylbenzoyl)-phenylphosphineoxide (Irgacure819) was purchased by Ciba, vinyl-terminated poly(dimethylsiloxane) (VT PDMS) with an average molecular weight of 25000 g mol^{-1}, 3-mercaptopropyltriethoxysilane (MPTS), and diethylamine were supplied by Aldrich.

2.2. Methods. *2.2.1. Synthesis of Oleic Acid-Capped TiO_2 Nanorods.* Oleic acid-capped TiO_2 NRs were synthesized with a diameter of 3−5 nm and length of ca. 20 nm under nitrogen atmosphere using a standard air free technique, starting from dried and degassed reactants. The synthesis of the NRs occurs at low temperature (80−100 °C), by hydrolysis of the TTIP precursor in OLEA surfactant, and in an excess of the aqueous TMAO base solution which catalyzes polycondensation reaction of the precursor.[23] The as-prepared TiO_2 NRs were isolated from the reaction mixture and purified, by a solvent nonsolvent precipitation method by using methanol as nonsolvent and then dispersed in chloroform or hexane.

2.2.2. Capping Exchange of Oleic Acid-Capped TiO_2 NRs with 3-(Trimethoxysilyl)propyl Methacrylate. Pristine OLEA ligand molecules (see Scheme 1) of the TiO_2 NRs were partially replaced by using MEMO as new capping agent following, with minor modifications, the procedure reported by De Palma et al.[26] Briefly, the treatment was performed by washing OLEA-capped TiO_2 NRs by several cycles of dispersion in ethanol and isolation by centrifugation, in order to remove the excess of OLEA coordinated to the surface of the nanoobjects. After such a treatment, the powder of NRs was dispersed in hexane and MEMO was added with 1:10 TiO_2/MEMO molar ratio. Finally, acetic acid was added in a 1:3 MEMO/acetic acid molar ratio for catalyzing silanization of MEMO at the NR surface, and the solution was left to stir overnight. During the treatment process, the color of the stirring solution turns gradually from transparent to opaque, likely due to aggregation of the OLEA/MEMO-coated TiO_2 NRs in hexane, indicating that a change in the NR surface chemistry has effectively occurred. Then, OLEA/MEMO-capped TiO_2 NRs were purified by means of two cycles of dispersion in ethanol and isolation by centrifugation, to remove MEMO in excess and residual OLEA.

Scheme 1. Molecular Structure of the Formulation Components and Capping Ligands

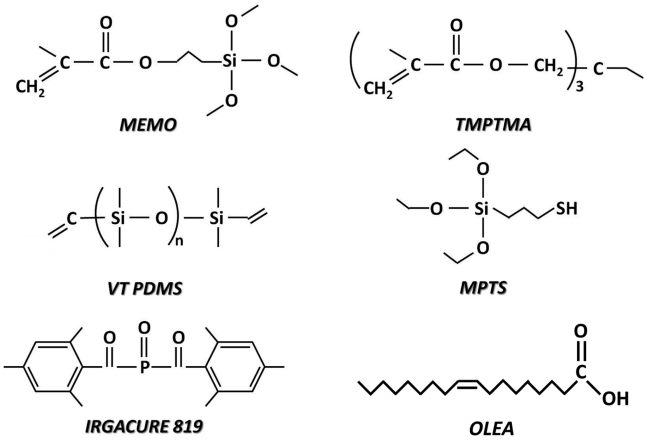

2.2.3. Preparation of the Photocurable Resin Formulation. The investigated UV-curable methacrylic-siloxane resin was based on a mixture of prepolymers, namely, MEMO, TMPTMA, and VT PDMS, the last modified with MPTS (Scheme 1). VT PDMS has been functionalized with MPTS because of its ability in limiting the inhibition effect of oxygen on the free-radical photopolymerization reactions and hence is then indicated as m-VT PDMS, following a route comprehensively illustrated in a previous study.[9] The functionalization was performed by mixing the two components at 100 °C in a 1:1 molar ratio in the presence of 1 wt % diethylamine.[9]

TMPTMA was added to m-VT PDMS and left to stir in an oil bath at 60 °C for 1 h. TMPTMA was chosen as the main thermosetting polymeric component for its high reactivity and low viscosity (45 mPa·s at 25 °C). Finally, MEMO was added to the mixture of TMPTMA and m-VT PDMS, and such a dispersion, photoinitiated with Irgacure819 in a content of 1 wt %, is here indicated as Photo_Resin (Table 1).

2.2.4. Preparation of Nanocomposite Formulations. OLEA/MEMO-coated TiO_2 NRs were dispersed in MEMO at a concentration of 1 wt % by stirring at room temperature and then added to the mixture of TMPTMA and m-VT PDMS and left to stir overnight. A preliminary incorporation of the OLEA/MEMO-capped TiO_2 NRs in neat MEMO was required in order to disperse the NRs in the more viscous m-VT PDMS and TMPTMA prepolymers.

Different samples were prepared and investigated in the work, and the whole series with related composition is shown in Table 1. Namely, two different formulations made of TiO_2 NR modified methacrylic-siloxane resin were prepared. The former nanocomposite formulation was added by Irgacure819 (1 wt %), and it is indicated as Photo_Nanocomposite; the latter was prepared by using the bare NR-based resin, and it is indicated as Nanocomposite (Table 1). Finally, samples based on bare resin with photoinitiator and bare resin without photoinitiator, indicated as Photo_ Resin and Resin (Table 1), respectively, were prepared as references.

2.3. Characterization. Steady state UV−vis absorption spectra were recorded with a Cary 5000 (Varian) UV/vis/near-IR spectrophotometer at room temperature.

Attenuated total reflection Fourier transform infrared (ATR-FTIR) spectra were used for collecting infrared spectra of the organic-coated TiO_2 NRs before and after capping exchange, by means of a PerkinElmer Spectrum One Fourier transform infrared spectrometer equipped both with a deuterated triglycine sulfate detector and a three-bounce, 4 mm diameter diamond microprism as internal reflection element. The measurements were performed by dropping aliquots (3−5 μL) of sample solutions directly onto the upper face of a diamond crystal, and spectra were acquired, with a resolution of 4 cm^{-1}, upon solvent evaporation.

TEM analysis was performed by using a Jeol Jem-1011 microscope, working at an accelerating voltage of 100 kV. TEM images were acquired by a Quemesa Olympus CCD 11 Mp camera. For collecting images of the OLEA- and OLEA/MEMO-capped TiO_2 NRs, the sample was prepared by dipping the 300 mesh amorphous carbon-coated Cu grid in a chloroform solution of the NRs and leaving the solvent to dry. For collecting TEM images of Nanocomposite, such a sample has been spin-coated at 8000 rpm for 30 s on a TEM grid and left exposed under a UV-lamp overnight for allowing curing of the methacrylic-siloxane resin. Statistical size analysis (NP average size and

Table 1. Composition of the Samples Investigated in the Work[a]

component (wt %)	Photo_MEMO	Photo_MEMO_NR	Photo_Resin	Photo_Nanocomposite	Resin	Nanocomposite
MEMO	99	98	84.2	83.3	85	84.2
TMPTMA			9.9	9.8	10	9.9
m-VT PDMS			4.9	4.9	5	4.9
IRGACURE 819	1	1	1	1		
OLEA/MEMO-TiO_2 NRs		1		1		1

[a]"Photo" prefix stands for Irgacure819-photoinitiated sample.

DOI: 10.1021/acsami.5b03731
ACS Appl. Mater. Interfaces 2015, 7, 15494−15505

size distribution) of the NPs was performed by the freeware ImageJ analysis program.

X-ray diffraction of the TiO_2 NR powder was collected by a PW 1729 Philips, using Cu Kα radiation in reflection mode (λ = 0.154 nm). The samples were step-scanned at room temperature from 2θ values of 10−60°.

Enthalpy involved in the UV-light-induced photopolymerization of samples was estimated by a photo differential scanning calorimeter (photo-DSC, Mettler Toledo DSC1 StareSystem) equipped by a 300 W xenon lamp Hamamatsu LC8 operating at a wavelength of 370 nm. Isothermal scans were run at 25 °C in either nitrogen or air atmosphere with a light radiation intensity of 3.7×10^{-2} $\mu W \cdot cm^{-2}$ and wavelength of the main line of 370 nm The experiments were stopped when no residual exothermal signal could be detected. Small samples (about 1 mg) were used in order to achieve isothermal conditions and a uniform degree of curing through sample thickness. The photocalorimetric experiments were replicated at least three times, and for each photo-DSC experiment, the sample was irradiated after 1 min from the beginning of the test. The tangent to the heat flow curve related to the first minute, when the sample was in the dark, was used as the baseline for peak integration. In addition, a baseline run was systematically performed before any test to rule out lamp heating effect.

In order to measure the residual reactivity and the glass transition temperature of the samples cured under UV light, dynamic DSC measurements were performed in nitrogen atmosphere on samples spin-coated on an aluminum crucible at 500 rpm for 30 s and exposed for 30 min to a UV lamp. The samples for dynamic DSC analysis were obtained by cutting the aluminum crucible in circular pieces of 4 mm in diameter. A dynamic DSC thermal scan has been preliminarily performed on a bare Al sample, in order to obtain a blank curve, to be subtracted from the DSC curves of the photocured films to evaluate the residual heat of reaction for each cured sample. Such a latter calculation has been performed by normalizing the heat of reaction, measured from DSC dynamic scan, with respect to the total weight of each sample, formed of the aluminum substrate and of the photocured film.

Thermal stabilities of OLEA- and OLEA/MEMO-coated TiO_2 NRs were measured by thermogravimetric analysis with a TGA/DSC1 Star and System (Mettler Toledo), and three replicas of each sample were investigated for increasing measurement accuracy. To this aim, the samples were heated from room temperature up to 1000 °C at 10 °C·min^{-1} in air atmosphere.

Transmittance Fourier transform infrared spectra were collected by a FT/IR-6300 Jasco instrument and used for investigating, upon UV-light exposure, the photopolymerization reaction. Such an analysis was performed on samples cast on KBr crystal and exposed for diverse times to a UV lamp having an irradiation intensity of 96 $mW \cdot cm^{-2}$ and wavelength of the main line of 365 nm

Dynamic contact angle measurements were performed on self-standing UV-cured samples with a First Ten Angstroms FTA1000 quick start instrument, equipped with a video camera. The analysis was performed at room temperature by means of the sessile drop technique and using as measuring liquid double-distilled water (surface tension γ = 72.1 $mN \cdot m^{-1}$).[28] Thirty measurements were carried out on each specimen, and the results were averaged.

3. RESULTS AND DISCUSSION

3.1. Surface Treatment of OLEA-Capped TiO_2 NRs with MEMO and Photopolymerization Kinetics of the TiO_2 NR Modified MEMO Mixture. Presynthesized TiO_2 NRs coated by OLEA ligand (Scheme 1) cannot be dispersed in the methacrylic-siloxane organic matrix due to their hydrophobic surface chemistry, and hence they have been surface-functionalized with the organofunctional silane 3-(trimethoxysilyl)propyl methacrylate (Figure 1, panel A).

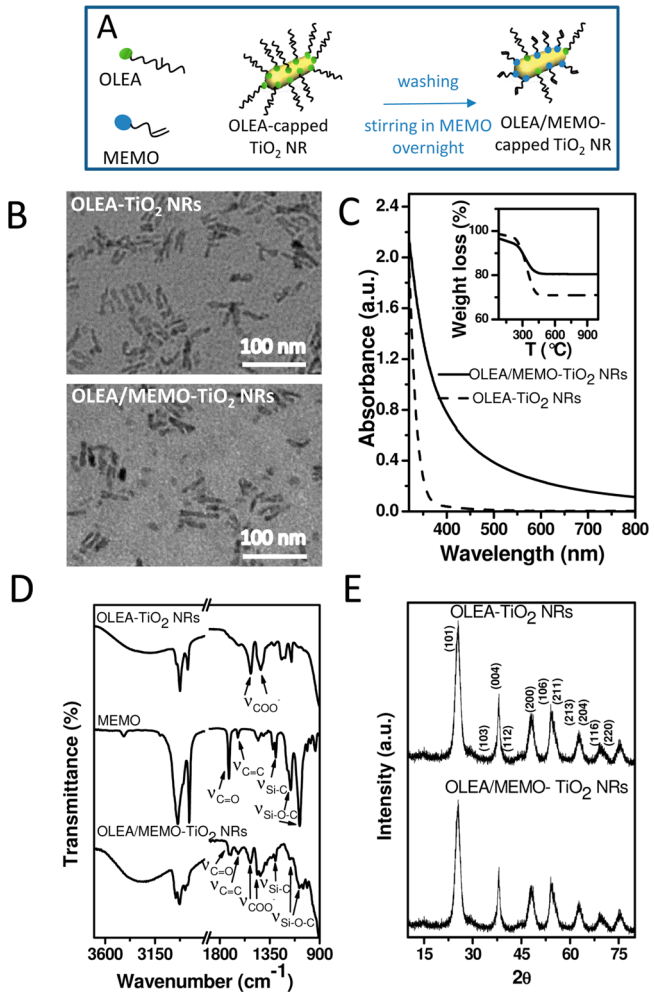

Figure 1. (A) Scheme of capping ligand exchange procedure. (B) TEM images of OLEA- and OLEA/MEMO-coated TiO_2 NRs. (C) UV−vis absorption spectra of OLEA- and OLEA/MEMO-capped TiO_2 NRs, 3 mM in $CHCl_3$ and *n*-PrOH, respectively. (Inset of C) TGA curves of OLEA- and OLEA/MEMO-coated TiO_2 NRs. (D) FTIR-ATR spectra of OLEA-capped TiO_2 NRs, neat MEMO, and OLEA/MEMO-coated TiO_2 NRs. (E) XRD patterns of OLEA- and OLEA/MEMO-capped TiO_2 NRs.

The picture of the vial containing MEMO-functionalized TiO_2 NRs shows their dispersibility in the medium, although the resulting dispersion appears slightly milky.

MEMO is expected to act as a coupling agent, able to covalently bind, by means of a silanization reaction,[20] hydroxyl groups at the NR surface[21] and to graft the NRs with reactive methacrylic functionalities. Such moieties are intended not only to make NR dispersible in the resin but also to promote, under UV exposure, cross-linking with the methacrylic-siloxane monomers of the formulation, improving even further dispersion in the host. In addition, MEMO is an amenable capping molecule due to its composition, which makes it less sensitive to photocatalytic degradation.

Spectroscopic, calorimetric, and microscopic investigation has provided relevant knowledge on morphology, crystalline structure and optical properties of the NRs, before and after capping exchange, and demonstrated their surface functionalization with MEMO molecules, confirming, at the same time, retention of the TiO_2 NR characteristics.

DOI: 10.1021/acsami.5b03731
ACS Appl. Mater. Interfaces 2015, 7, 15494−15505

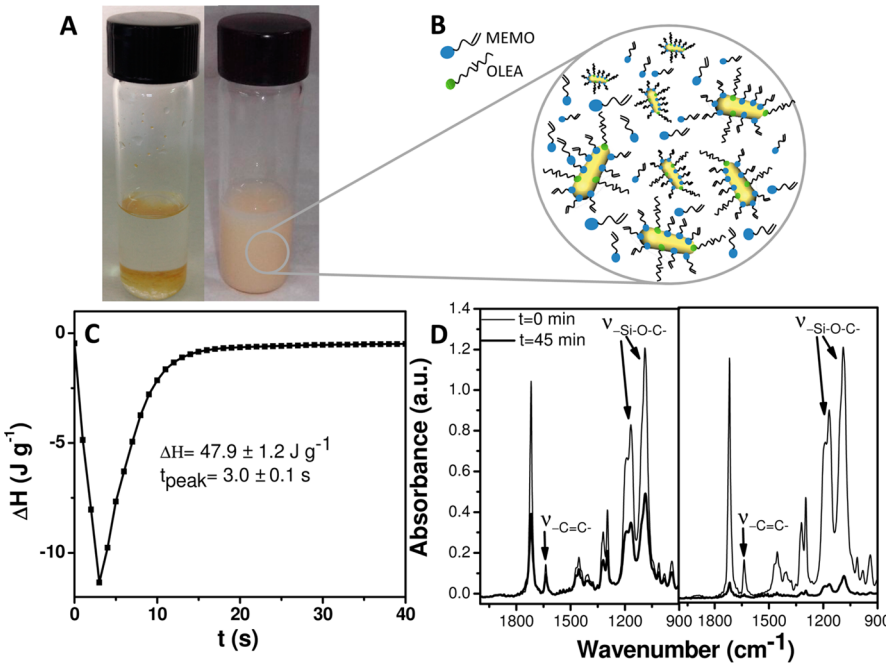

Figure 2. (A) Picture of (on the left) OLEA- and (on the right) OLEA/MEMO-capped TiO_2 NRs dispersed in MEMO. (B) Sketch of the structure of the dispersion of NRs in MEMO. (C) Photo-DSC thermogram of Photo_MEMO_NR formulation in air, heat of reaction ΔH (J g^{-1}) and corresponding time to reach the maximum of the peak t_{peak} (s) measured from the isothermal photo-DSC scan. (D) FTIR spectra of Photo_MEMO (left panel) and Photo_MEMO_NR (right panel) before and after 45 min of UV-light exposure.

Panel B of Figure 1 reports TEM images of OLEA- and OLEA/MEMO-capped TiO_2 NRs. These images show how the as-synthesized elongated NPs, having an average length up to 20 nm and diameter of 3−4 nm (as demonstrated by the statistical analysis reported in Figure S1 of the Supporting Information), appear rather well spaced and separated on the grid, because of the presence of the long alkyl chain OLEA molecules. After surface treatment with MEMO, the NPs preserved the elongated morphology as confirmed by the statistical data reported in Supporting Information Figure S2.

Panel C of Figure 1 displays UV−vis spectra of TiO_2 NRs, surface-coordinated by OLEA and surface-modified with OLEA/MEMO, respectively. Both spectra show the typical featureless line shape of high-band-gap TiO_2 semiconductor. Upon treatment with MEMO, the NRs display mainly the same spectral behavior, apart from a slight increase in the absorption baseline due to scattering effects caused by a moderate aggregation among NRs, as can be also seen from bare eye observation in Figure 1A. In the inset of panel B, a comparison of TGA curves of OLEA- and OLEA/MEMO-coated TiO_2 NRs is reported. The thermogravimetric analysis shows for the OLEA/MEMO-capped TiO_2 NRs a desorption temperature almost comparable to that of the OLEA-coated TiO_2 NRs, but a lower weight loss, that is 19% against 29%. The weight loss in TGA curves of organic-coated NPs is typically ascribed to oxidation and/or debonding and degradation of the organic layer at the NP surface and is directly correlated to the coverage of the coating layer coordinating the surface of the NPs.[29] In the case of silane molecules, the weight loss can be also related to the elimination of water molecules generated mainly from condensation of silanol groups, to form siloxane groups, and to a lesser extent, from the condensation reactions of remaining hydroxyl groups on the NP surfaces.[30] Thus, since the surface treatment of OLEA-capped TiO_2 NRs with MEMO has been performed upon cycles of purification of the nanoobjects from OLEA and then exposure to MEMO in excess, the surface of OLEA/MEMO-coated TiO_2 NRs presents a lower amount of OLEA ligand with respect to that of as-synthesized NRs, and hence such a result is consistent with the change of the NR surface chemistry that occurred upon treatment with MEMO.

In the case of silane molecules, the weight loss can be also related to the elimination of water molecules generated mainly from condensation of silanol groups, to form siloxane groups, and to a lesser extent, from the condensation reactions of the remaining hydroxyl groups on the NP surfaces.[30] Thus, since the surface treatment of OLEA-capped TiO_2 NRs with MEMO has been performed upon cycles of purification of the nanoobjects from OLEA and then exposure to MEMO in excess, the surface of OLEA/MEMO-coated TiO_2 NRs presents a lower amount of OLEA ligand with respect to that of as-synthesized NRs, and hence, such a result is consistent with the change of the NR surface chemistry that occurred upon treatment with MEMO.

Finally, FTIR-ATR analysis provides a concluding assessment of such a surface modification. Panel C of Figure 1 reports FTIR spectra of pristine OLEA-coated TiO_2 NRs, neat MEMO, and OLEA/MEMO-capped TiO_2 NRs. The spectrum of OLEA/MEMO-capped TiO_2 NRs shows in the low wavenumber spectral region typical vibrations of silane; namely, at 1716 and 1633 cm^{-1} the stretching vibrations of conjugated esteric -C═O and -C═C- moieties, at 1295 cm^{-1} the stretching signals of -Si−C- and at 1160 and 1079 cm^{-1} the -Si−O−C- stretching of MEMO can be noticed.[26] A partial retention of the pristine OLEA ligand molecules is pointed out by the presence of peaks at 1521 and 1430 cm^{-1} ascribed to the antisymmetric and symmetric -COO^- stretching, respectively, of OLEA, coordinated to surface Ti atoms through a bidentate bond.[23] On the other hand, the high-wavenumber region of the infrared spectrum of OLEA/MEMO-capped TiO_2 NRs is characterized by the vibrations at 2962 and at 2877 cm^{-1},

DOI: 10.1021/acsami.5b03731
ACS Appl. Mater. Interfaces 2015, 7, 15494−15505

attributed to asymmetric and symmetric stretching of -CH_3, respectively, and by signals at 2927 and at 2852 cm^{-1} assigned to asymmetric and symmetric stretching of -CH_2-, respectively, typical of both MEMO and residual OLEA. The presence of -Si−O−C- vibrations in OLEA/MEMO-capped TiO_2 NRs indicates an incomplete hydrolysis and condensation of the silane molecules during ligand exchange, to the hydroxyl moieties at the NR surface. Finally, the appearance of a band at 1049 cm^{-1} typical of -Si−O−Si- vibrations is due to formation of silane layers at the surface of the silane-coated NRs.[26]

X-ray diffraction spectra of OLEA- and of OLEA/MEMO-capped TiO_2 NRs are finally reported in panel D of Figure 1. The picture shows for both samples the characteristic line broadening of diffraction peaks of nanosized crystalline domains. In particular, XRD profiles of both the TiO_2 NR samples clearly present a very intense peak for the (101) reflex, while less intense and narrower are the peaks corresponding to the (004) and (200), (211) and (220) reflexes. Such features are accounted for by the NR anisotropy, as a preferred growth orientation takes place along the (101) direction, that is the *c*-axis of the anatase lattice.[23] Therefore, after MEMO grafting at the NR surface, their pristine anatase phase is preserved, along with its anisotropy.

MEMO has been used as a "common solvent" for dispersing the NRs in the more viscous components of the organic formulation, namely, TMPTMA and m-VT PDMS (Scheme 1), in a concentration of 1 wt %. Panel A of Figure 2 reports a picture of the corresponding dispersion demonstrating how the change in NR surface chemistry has definitely improved their chemical affinity with the MEMO component (Figure 2, panel B).

A first kinetic study has been performed in order to evaluate a possible effect of the incorporation of TiO_2 NRs on photopolymerization of MEMO by carrying out photo-DSC and FTIR spectroscopy analysis on a mixture of MEMO and TiO_2 NRs and on neat MEMO, respectively, both added with Irgacure819 as photoinitiator (Scheme 1). These samples are indicated as Photo_MEMO and Photo_MEMO_NR (Table 1), respectively.

Isothermal photo-DSC analysis performed on Photo_-MEMO in air does not show any significant reaction peak (data not shown): in fact the sample appears still completely liquid after the whole scan. Such evidence is consistent with the relevant literature in the field, as the rate of the MEMO photopolymerization reaction is reported to be very low in air atmosphere.[8] Therefore, no heat can be detected for such a reaction, when a low power UV lamp, such as that operating in the photo-DSC, is used.[8] This behavior can be ascribed to oxygen inhibition of free-radical photopolymerization reaction, responsible for a series of detrimental effects, including slow polymerization rate, long induction period, low conversion rate, short polymeric chain length, and detrimental mechanical properties (i.e., scratch resistance, hardness, T_g, and transparency).[31]

Interestingly, a peak ascribable to a photopolymerization reaction (Figure 2, panel C) is present in the average photo-DSC thermogram of the Photo_MEMO_NR sample. In particular, the value of the heat released during photopolymerization of Photo_MEMO_NR and the time to reach the peak maximum, both estimated by the isothermal photo-DSC analysis in air atmosphere, result in 47.2 ± 1.2 $J \cdot g^{-1}$ and 3 s, respectively (Figure 2, panel C). This evidence indicates that the incorporation of TiO_2 NRs is able to catalyze a fast UV-light-induced curing of MEMO in air.

In panel D of Figure 2 the fingerprint regions of FTIR spectra of Photo_MEMO and Photo_MEMO_NR, collected before and after 45 min of UV-light exposure, are reported.

The FTIR spectra of Photo_MEMO and Photo_MEMO_NR show the same line shape before UV illumination, the peaks being observed in the spectra mainly assigned to the most abundant component of both samples, that is, MEMO. In particular, the spectra present, in the low-wavenumber region, namely, at 1637 cm^{-1}, the stretching vibrations of methacrylic -C═C- along with the typical -Si−O−C- stretching modes of MEMO at 1160 and 1079 cm^{-1}. On the other hand, in the high-wavenumber region typical asymmetric and symmetric stretching modes of -CH_2 at 2841 and at 2945 cm^{-1}, respectively, and the shoulder of the symmetric stretching of -CH_3 moieties of MEMO at 2897 cm^{-1} (data not shown) are present.

After UV-light irradiation, no new peak is noticed either in the spectra of Photo_MEMO or in those of Photo_-MEMO_NR, while a decrease of intensity of all of the peaks is observed in the spectra of both samples, much more for Photo_MEMO_NR with respect to Photo_MEMO.

In addition, the lack of bands corresponding to -Si−O−Si- vibrations, expected between 1130 and 1000 cm^{-1},[26] reasonably allows one to exclude the occurrence of silanization reaction of the -Si−O−C- functionalities of MEMO, either in Photo_-MEMO_NR and in Photo_MEMO.

Interestingly, while under UV light the cross-linking reaction of methacrylic -C═C- in the Irgacure819 containing MEMO is not expected in the applied experimental conditions;[8] when TiO_2 NRs are added to such a sample, the photoactivity of the nanooxide[24] is found to promote cross-linking reactions among the methacrylic -C═C- groups of MEMO. Such a result can be inferred through the observation of the UV-light-induced conversion of methacrylic -C═C- moieties into alkylic groups in Photo_MEMO_NR with respect to Photo_MEMO, which has been calculated considering the intensity of the most intense -Si−O−C- vibration, at 1079 cm^{-1}, being constant and assuming such a signal as a reference for normalizing the intensity of the methacrylic -C═C- peak (at 1637 cm^{-1}) of the corresponding spectrum. The ratio between the normalized values of Photo_MEMO and Photo_MEMO_NR has been found to steadily increase, reaching more than 60% after 45 min of UV-light illumination.

Such a study finds evidence of the reaction of methacrylic -C═C- moieties in Photo_MEMO_NR induced by the embedded TiO_2 NRs, otherwise not occurring in the bare Photo_MEMO, thus confirming the photoactivation/photo-initiation effect of the TiO_2 NRs on the Irgacure819-containing MEMO sample.

3.2. Photopolymerization Kinetic of Formulations Added with Irgacure819. The interesting behavior of TiO_2 NRs in curing MEMO and in promoting conversion of its methacrylic moieties prompts us to investigate the photopolymerization kinetic of the whole methacrylic-siloxane formulation. The formulation design has taken into account that TiO_2 NRs can induce photocatalytic degradation of a polymer matrix. Indeed, a low NR loading has been used, and a high content (85% by weight) of the methacrylic-based silane MEMO has been considered, while, correspondingly, the amount of TMPTMA and m-VT PDMS has been kept low (Table 1).

DOI: 10.1021/acsami.5b03731
ACS Appl. Mater. Interfaces 2015, 7, 15494−15505

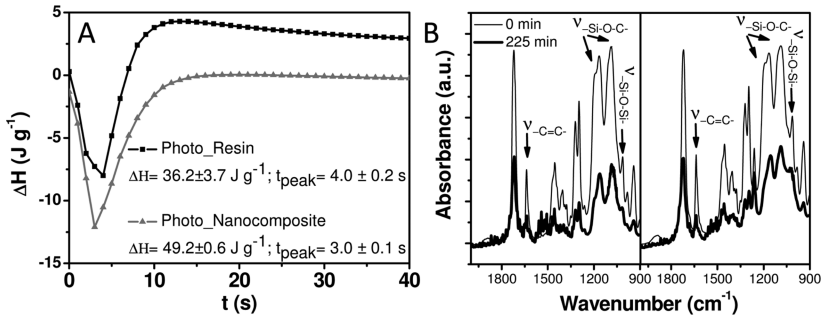

C

Sample	$\Delta H_{residual}$ (J g^{-1}) I scan	$\Delta H_{residual}$ (J g^{-1}) II scan
Photo_Resin	12.4 ± 0.7	0
Photo_Nanocomposite	1.6 ± 0.1	0

Figure 3. (A) Photo-DSC thermograms of Photo_Resin and Photo_Nanocomposite formulations in air atmosphere. (B) FTIR spectra of Photo_Resin (left panel) and Photo_Nanocomposite (right panel) before and after 225 min of UV-light exposure. (C) Residual heat of reaction ($\Delta H_{residual}$), normalized with respect to the weight of the neat resin, estimated by thermal dynamic DSC curves referred to first and second scans, respectively.

Photo-DSC analysis has been carried out, in air, on Photo_Nanocomposite along with the corresponding reference sample of Photo_Resin, without TiO_2 NRs (Table 1). The heat flow estimated by the photo-DSC analysis has been used to compare curing reactivity of both systems, since the heat released during photopolymerization is proportional to the curing capability.[32]

In panel A of Figure 3, the photo-DSC thermograms of Photo_Resin and Photo_Nanocomposite are reported. The heat of reaction (ΔH) and time to reach the maximum of the reaction peak (t_{peak}) for both formulations have been estimated from the corresponding photo-DSC isothermal curves.

The experimental data clearly show that the time to reach the peak maximum of the TiO_2 NR loaded formulation is very low (about 3−4 s), and it is comparable with that of the neat organic formulation photoinitiated by Irgacure819.[8]

The heat measured for the UV-light-induced reaction of the nanocomposite, in air, calculated by normalizing the total enthalpy to the weight of sole organic content, has been found to increase about 26% in comparison to that measured for the bare resin, under the same experimental conditions. Such an increase of exothermicity can be explained in terms of a higher conversion degree and, thus, a higher cross-linking density of the photocurable formulation, which can be only attributed to the embedded TiO_2 NRs.

The increased reactivity of the photopolymerizable formulation containing 1 wt % of TiO_2 NRs has been observed also in DSC dynamic thermal analysis performed on UV-light-cured spin-coated films of Photo_Resin and Photo_Nanocomposite. Residual heat of reaction, $\Delta H_{residual}$, measured after the first and second thermal dynamic DSC scans respectively are reported in panel C of Figure 3. The thermal DSC results further point out the extraordinarily beneficial effect of TiO_2 NRs on the free-radical photopolymerization of the UV-curable resin, since residual heat of reaction measured after curing of the mixtures in air for 30 min decreases from 12.4 J·g^{-1} for the bare resin, to 1.6 J·g^{-1} for the 1 wt % NR based nanocomposite, hence dropping 87%, thus demonstrating that the NRs limit the inhibition effect of oxygen on the photopolymerization process. Upon a subsequent thermal DSC scan no residual heat of reaction has been detected for both Photo_Resin and Photo_Nanocomposite, thus pointing out that the reaction is complete after the first DSC scan for both of the analyzed samples.

Panel B of Figure 3 reports the fingerprint region of FTIR spectra of Photo_Resin and Photo_Nanocomposite, before and after 225 min of UV-light exposure. As it can be noticed, the FTIR spectra of Photo_Resin and Photo_Nanocomposite present the same line shape before UV-light illumination, the peaks being observed in the spectra mainly ascribed to the monomers of the formulation, which are TMPTMA, MEMO, and m-VT PDMS (Table 1).

The spectra are characterized in the low-wavenumber region by -C═C- stretching vibrations of TMPTMA, MEMO, and m-VT PDMS at 1638 cm^{-1}, by -Si−O−C- modes of MEMO and MPTS at 1165 and 1088 cm^{-1}, respectively, and by -Si−O−Si- vibrations of m-VT PDMS at 1012 cm^{-1}. In the high-wavenumber region, the stretching of methacrylic and vinyl groups of TMPTMA, MEMO, and m-VT PDMS at 3104 cm^{-1}, along with the asymmetric and symmetric -CH_2 stretching at 2841 and at 2946 cm^{-1}, respectively, and the shoulder of the symmetric -CH_3 stretching at 2897 cm^{-1} of MEMO, TMPTMA, and m-VTPDMS can be observed (data not shown).

Upon UV-light irradiation, no new peak has been detected either in the spectra of Photo_Resin or in those of Photo_Nanocomposite, while a decrease of intensity of all of the peaks is observed for both samples. In addition, both in Photo_Resin and in Photo_Nanocomposite, the intensity of the -Si−O−Si- mode observed at 1012 cm^{-1}[26] does not change, and thus the silanization reaction of the -Si−O−C- functionalities can be excluded.

Interestingly, under UV light, when TiO_2 NRs are added to the Irgacure819-containing Resin (Photo_Resin) sample, the photoactivity of the nanooxide[24] is found to promote cross-linking reactions among the methacrylic -C═C- groups of formulation components. Such a result can be explained by the study of the UV-light-induced conversion of methacrylic -C═C- moieties into alkylic groups in Photo_Nanocomposite with respect to Photo_Resin, which has been calculated considering the intensity of the most intense -Si−O−C- vibration, at 1088 cm^{-1}, being constant and assuming such a signal as a reference

DOI: 10.1021/acsami.5b03731
ACS Appl. Mater. Interfaces 2015, 7, 15494−15505

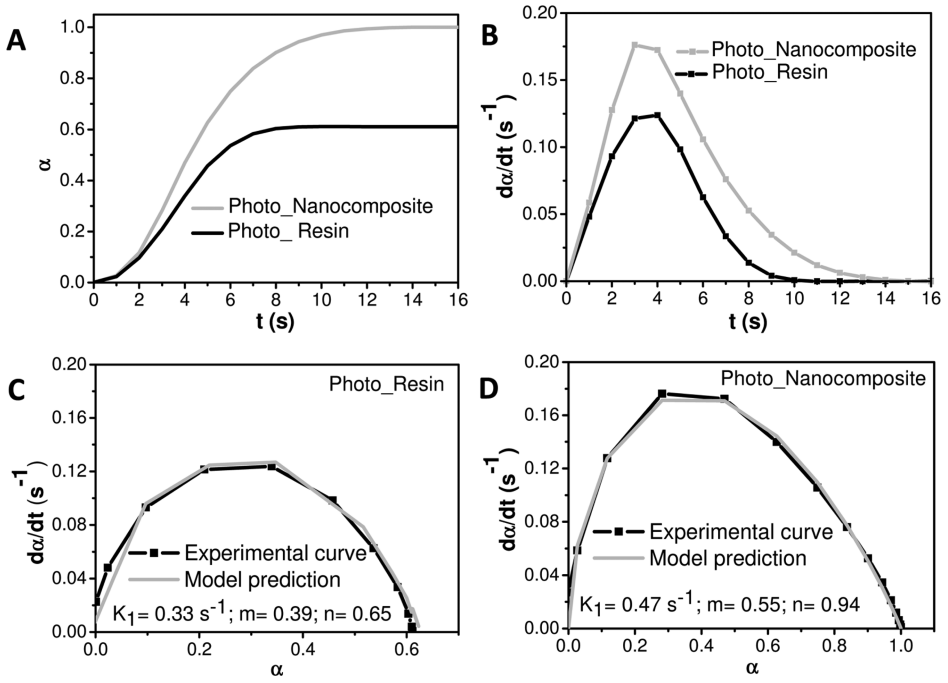

Figure 4. (A) Extent of reaction versus time and (B) reaction rate versus time for Photo_Resin and Photo_Nanocomposite. (C, D) Comparison between experimental data and kinetic model prediction for Photo_Resin (C) and Photo_Nanocomposite (D). In C and D kinetic parameters of the curing reaction were achieved by using eq 2.

for normalizing the intensity of the methacrylic -C═C- peak (at 1638 cm^{-1}) of the corresponding spectrum.

The ratio between the normalized values of Photo_Resin and Photo_Nanocomposite has been found to be steadily enhanced, reaching more than 70% after 225 min of UV-light illumination corresponding to an exposure dose of 1296 J cm^{-2}. This result points out the increased cross-linking of methacrylic -C═C- moieties of the formulation when loaded by TiO_2 NRs.

Photo-DSC measurements have been carried out to monitor advancement of the cross-linking reaction, taking into account that the heat evolved at a defined time is proportional to the reactive groups consumed, with the result thus being related to the extent of reaction.[33] The extent of reaction, α, can be, therefore, defined as[8]

$$\alpha = \frac{H(t)}{H_{max}} \tag{1}$$

where $H(t)$ is the heat of reaction developed at time t during an isothermal photo-DSC experiment and H_{max} is the maximum heat of reaction obtained from the same photo-DSC experiment.

The value of α as a function of reaction time is reported in Figure 4 (panel A) for both systems. The α curves confirm that a higher photopolymerization conversion is achieved in shorter reaction time for the formulation containing the OLEA/MEMO-coated TiO_2 NRs with respect to the reference sample. Remarkably, a 100% final conversion has been found for the reaction of Photo_Nanocomposite in air, while for the reference system the conversion has resulted in only 60%.

The photopolymerization kinetics in isothermal mode of Photo_Nanocomposite and Photo_Resin has been also investigated, considering a simple n-order kinetic equation, as first proposed by Maffezzoli and Terzi[33] for free-radical polymerization of unsaturated polyester and acrylic matrix composites for dental applications:

$$\frac{d\alpha}{dt} = K_1\alpha^m(1-\alpha)^n \tag{2}$$

where K_1 is a temperature-dependent rate constant and n and m are positive setting parameters which do not depend on temperature and give an indication of the kinetic order of reaction. The constant K_1 represents the initial rate of reaction, and it takes into account the autocatalytical effects of the theoretical model prediction of eq 2.

The reaction rate, $d\alpha/dt$, can be calculated from the heat flow dH/dt as[33]

$$\frac{d\alpha}{dt} = \frac{1}{\Delta H_{max}}\frac{dH}{dt} \tag{3}$$

where the maximum heat of reaction, ΔH_{max}, has been calculated as previously explained.

The reaction rate ($d\alpha/dt$) curves of Photo_Resin and Photo_Nanocomposite have been calculated starting from the conversion curves reported in panel A of Figure 4 (see panel B of Figure 4). In addition, panels C and D compare the experimental and theoretical curves obtained for both systems in air atmosphere, along with the kinetic data fitted using eq 2.

The kinetic parameters obtained for both systems at 30 °C and light intensity of 3.7×10^{-2} $\mu W \cdot cm^{-2}$ (panels C and D of Figure 4) confirm the higher reactivity and cure rate of the formulation containing the OLEA/MEMO-coated TiO_2 NRs, the kinetic constant K_1 being mainly affected by autocatalytic phenomena and orders of reaction m and n being higher than those found for Photo_Resin.

3.3. Photopolymerization Kinetic of Formulations with and without TiO_2 NRs. Taking into account the extraordinary increase of reactivity of the methacrylic-siloxane-based nanocomposite containing just 1 wt % NRs, the possibility to cure the formulation without addition of Irgacure819, but using only a suitable amount of OLEA/

DOI: 10.1021/acsami.5b03731
ACS Appl. Mater. Interfaces 2015, 7, 15494−15505

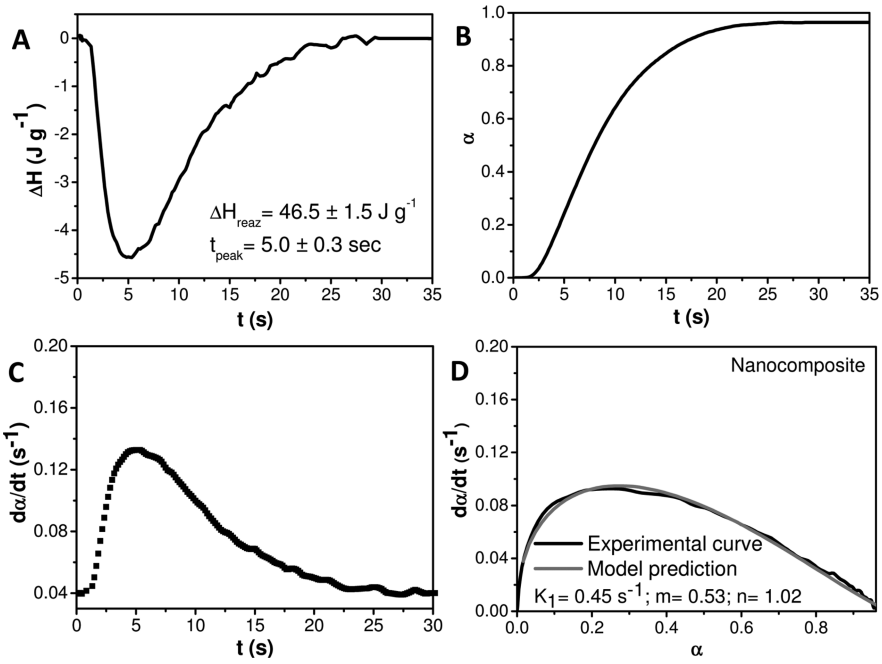

Figure 5. (A) Photo-DSC thermograms of nanocomposite formulation in air atmosphere. (B) Extent of reaction versus time, (C) reaction rate versus time, and (D) comparison between experimental data and kinetic model prediction for nanocomposite with kinetic parameters of the curing reaction achieved by using eq 2.

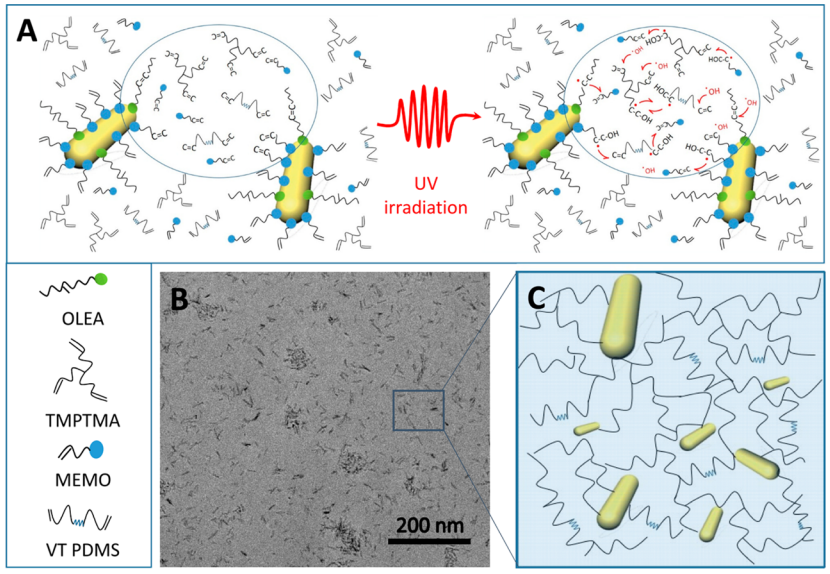

Figure 6. (A) Sketch of photopolymerization reactions of the curable resin formulation loaded with OLEA/MEMO-coated TiO_2 NRs. (B) TEM image of nanocomposite. (C) Sketch of the nanocomposite structure upon curing.

MEMO-capped TiO_2 NRs, has been evaluated. For this purpose, two formulations based on neat resin and nanocomposite, both prepared without Irgacure819 (Nanocomposite and Resin (Table 1)) have been characterized by photo-DSC analysis.

A first isothermal photo-DSC scan has been performed in air on both formulations, and only in case of Nanocomposite has a DSC peak been observed (Figure 5). Indeed, the neat organic formulation without NRs, namely, Resin, has been found completely liquid after the photo-DSC scan and no DSC peak has been detected, thus indicating that such a formulation could not photopolymerize.

The results show that the heat of reaction of Nanocomposite measured from the DSC curve of Figure 5 (46.5 ± 1.5 J·g^{-1}) is significantly higher than that measured for the neat resin formulation photoinitiated by Irgacure819, i.e., Photo_Resin (36.2 ± 3.7 J·g^{-1}; see Figure 3) and comparable with that of the Photo_Nanocomposite sample (49.2 ± 0.6 J·g^{-1}; see Figure 3), while for all of the samples the time to reach the peak maximum is almost the same. In addition, the second thermal dynamic DSC scan performed on the Nanocomposite sample is evidence for a negligible residual heat of reaction of ca. 0.5 ± 0.1 J·g^{-1}, much lower than that measured for Photo_Resin (12.4 ± 0.6 J·g^{-1}; see Figure 3) and for Photo_Nanocomposite (1.6 ± 0.1 J·g^{-1}; see Figure 3).

DOI: 10.1021/acsami.5b03731
ACS Appl. Mater. Interfaces 2015, 7, 15494−15505

The kinetic parameters of Nanocomposite achieved by Photo-DSC experiments are reported in Figure 5. The extent of reaction, α, of Nanocomposite as a function of reaction time, estimated from eq 1 (Figure 5, panel B), shows a 100% final conversion in air atmosphere comparable with that of Photo_Nanocomposite (Figure 4, panel A), but higher than that of Photo_Resin (Figure 4, panel A). Remarkably, the reaction rate ($d\alpha/dt$) of Nanocomposite (Figure 5, panel C) along with the kinetic constant K_1 and order parameters n and m (Figure 5, panel D) are 0.45 s^{-1}, 0.53, and 1.02, thus higher than those of Photo_Resin (Figure 4, panels B and C), i.e., 0.33 s^{-1}, 0.39, and 0.65 and comparable with that of Photo_-Nanocomposite, namely, 0.47 s^{-1}, 0.55, and 0.94. This finding definitely demonstrates the extraordinary capability of the photoactive OLEA/MEMO-capped TiO_2 NRs in inducing photopolymerization of the formulation in air and under UV-light radiation with performance higher than that recorded for commercial photoinitiator Irgacure819. In particular, a higher exothermicity, a lower residual heat of curing, and higher values for kinetic parameters recorded for the Nanocomposite demonstrate its ability to self-cure, without a subsequent heat treatment, and thus with a lower inhibition effect of oxygen, and with a higher reactivity and cross-linking density than those achieved when Irgacure819 is used as photoinitiator, in the absence of NRs.

The capability of the NRs to photoinitiate the curing reaction can be explained by considering that, under UV-light illumination in air, photogenerated electron−hole pairs at the NR surface promote redox processes, which lead to the formation of hydroxyl radicals,[24] that generate radicals both on MEMO and residual OLEA molecules coordinated to the NR surface[34] (Figure 6, panel A).

Such reactive species can intercalate polymer chains and react by UV-induced radical processes with the monomers of the resin[6] formulation, i.e., MEMO, TMPTMA, and m-VT PDMS, thus providing cross-linking reactions that lead to networking of the NRs within the resin (Figure 6, panel A).

Panel B of Figure 6 shows that the embedded NRs retain morphology upon embedding in the photocurable matrix, as also demonstrated by the statistical analysis reported in Figure S3 of the Supporting Information, and confirms the almost uniform dispersion of the NRs in the organic matrix along with the limited interparticle aggregation after photopolymerization.

Incorporation of the NRs in the polymer matrix has been found to increase T_g along with the WCA of the organic formulation. Indeed, the T_g value estimated from the DSC thermal scan and the measured WCA pass from ca. 49 °C and 104° for Photo_Resin to 60 °C and 110° for Photo_-Nanocomposite and further increase to 65 °C and 114° for Nanocomposite, respectively (see Table 2). Such an increase in T_g and WCA values can be ascribed to the occurrence of multiple covalent interactions between the capping ligands of the NRs and the curable matrix which lead to a decrease of segmental mobility of polymer chains in the matrix,[32] thus limiting hydrophilic recovery of the sylanolic moieties at the polymer surface.[35] High-T_g values grant a high adhesion of the polymer material to inorganic surfaces, also when the coating absorbs water and moisture, since high-T_g value compensates plasticization effects.[36] Finally, it is worthwhile to notice that the highest T_g and WCA values of Photo_Nanocomposite and Nanocomposite samples confirm the capability of OLEA/MEMO-coated TiO_2 NRs in increasing the cross-linking density of the resin.

Table 2. Estimated Glass Transition Temperature (T_g) and Water Contact Angle (WCA) Values

sample	T_g (°C)	WCA (deg)
Photo_Resin	49 ± 10	104 ± 5
Photo_Nanocomposite	60 ± 8	110 ± 4
nanocomposite	65 ± 8	114 ± 4

4. CONCLUSIONS

A novel nanocomposite based on TiO_2 nanorods (NRs) surface coordinated by oleic acid (OLEA) and a methacrylic-silane ligand, MEMO, embedded in a UV-light-curable methacrylic-siloxane organic formulation, has been manufactured. The surface treatment of OLEA-capped TiO_2 NRs, prepared by a colloidal chemistry route, with MEMO coupling agent, improves NR dispersion in the organic formulation, being able to graft a NR surface with -C═C-groups which can react with the methacrylic moieties of the resin. The results show that the NRs retain anisotropic morphology and crystalline phase after treatment with the silane which covalently coordinates the nanoobjects by silanization with -OH groups located at the NR surface. The monomer precursor of the resin, that is, MEMO, has been used as a common dispersing medium for incorporating the NRs into the more viscous components of the formulation, increasing stability of the nanofillers and limiting their aggregation.

The curing ability of the resin formulation has been retained after incorporation of the OLEA/MEMO-coated TiO_2 NRs. In addition, under UV-light irradiation and in air atmosphere, TiO_2 NRs behave as photocatalyst of the polymerization process more effectively than the typical standard photoinitiator of the formulation, showing higher curing reactivity and cross-linking density and limiting inhibition effect of oxygen on the free-radical photopolymerization. Indeed, under UV-light irradiation the OLEA/MEMO-coated TiO_2 NRs promote the formation of hydroxyl radicals which react both with the -C═C- moieties of MEMO and residual OLEA capping molecules and the methacrylic groups of the formulation components promoting radicals which lead to cross-linking reactions. The multiple covalent interactions occurring among the capping ligand molecules coordinating the NR surface and the organic matrix provide a uniform dispersion of the nanofillers in the resin, hence increasing glass transition temperature (T_g) and water contact angle (WCA) of the polymer.

The opportunity to greatly accelerate the reactivity of a curable formulation when adding very small amounts of OLEA/MEMO-coated TiO_2 NRs and to accomplish completely the photopolymerization in environmental conditions after a short curing step (in the range of minutes) makes the nanocomposite a high-added-value material appealing for industrial-scale applications.

However, while the surface treatment of the TiO_2 NRs with MEMO, the low NR loading, and the high content of silane MEMO in the formulation should minimize risk of photocatalytic degradation of the host matrix, further investigation is needed to assess possible long-term photocatalytic damage due to prolonged light exposure.

The novel nanocomposite material can be interesting as hydrophobic, self-initiated coating for protecting monuments and artworks and for manufacturing denture components and optical elements. A further and next step can be to test the

DOI: 10.1021/acsami.5b03731
ACS Appl. Mater. Interfaces 2015, 7, 15494−15505

biocompatibility, UV-shielding properties and photocatalytic functionalities of the nanocomposite or optimize the loading of TiO_2 NR filler for transferring to the resin such properties, with the aim to manufacture a water-repellent, biocompatible, and autoinitiated coating which can be concomitantly UV-shielding and self-cleaning.

The approach implemented in this work, that is, grafting the surface of colloidal NRs by a silane coupling agent, can be extended to colloidal NCs having diverse chemical composition (metal, oxide, and chalcogenides); hence, diverse interesting properties (semiconductivity, luminescence, and magnetism) and to different curable resin (i.e., epoxy resin), thus opening the venue to the development of novel curable nanocomposite formulations, with a relevant potential for a wide range of technological applications, including solar cells, medical elements, electronic devices, sensors, and mechanically responsive components.

■ ASSOCIATED CONTENT

Ⓢ Supporting Information

Statistical analysis of average size and corresponding size distribution of TiO_2 NRs "as synthesized", OLEA/MEMO-coated, and OLEA/MEMO-coated incorporated in UV-cured organic formulation. The Supporting Information is available free of charge on the ACS Publications website at DOI: 10.1021/acsami.5b03731.

■ AUTHOR INFORMATION

Corresponding Author

*Tel.:+3908054442027. Fax: +390805442128. E-mail: lucia.curri@ba.ipcf.cnr.it.

Notes

The authors declare no competing financial interest.

■ ACKNOWLEDGMENTS

The work has been partially supported by the EC-funded Seventh FP Project LIMPID (Grant No. 310177), by PRIN 2012 (Protocol 20128ZZS2H) and MAIND "Materiali eco-innovativi e tecnologie avanzate per l'Industria Manifatturiera e delle costruzioni" (PON03PE_00004") Italian National projects. Mr. Donato Cannoletta is kindly acknowledged for his help in XRD data collection.

■ REFERENCES

(1) Hanemann, T.; Szabó, D. V. Polymer-Nanoparticle Composites: From Synthesis to Modern Applications. *Materials* **2010**, *3*, 3468–3517.

(2) Liu, H.; Webster, T. J. Mechanical Properties of Dispersed Ceramic Nanoparticles in Polymer Composites for Orthopedic Applications. *Int. J. Nanomed.* **2010**, *5*, 299–313.

(3) Bauer, F.; Flyunt, R.; Czihal, K.; Buchmeiser, M. R.; Langguth, H.; Mehnert, R. Nano/Micro Particle Hybrid Composites for Scratch and Abrasion Resistant Polyacrylate Coatings. *Macromol. Mater. Eng.* **2006**, *291*, 493–498.

(4) Lee, W. K.; Dai, Z.; King, W. P.; Sheehan, P. E. Maskless Nanoscale Writing of Nanoparticle-Polymer Composites and Nanoparticle Assemblies using Thermal Nanoprobes. *Nano Lett.* **2010**, *10*, 129–133.

(5) Ingrosso, C.; Fakhfouri, V.; Striccoli, M.; Agostiano, A.; Voigt, A.; Gruetzner, G.; Curri, M. L.; Brugger, J. An Epoxy Photoresist Modified by Luminescent Nanocrystals for the Fabrication of 3D High-Aspect-Ratio Microstructures. *Adv. Funct. Mater.* **2007**, *17*, 2009–2017.

(6) Ingrosso, C.; Martin-Olmos, C.; Llobera, A.; Innocenti, C.; Sangregorio, C.; Striccoli, M.; Agostiano, A.; Voigt, A.; Gruetzner, G.; Brugger, J.; Perez-Murano, F.; Curri, M. L. Oxide Nanocrystals based Nanocomposite for Fabricating Photoplastic AFM Probes. *Nanoscale* **2011**, *3*, 4632–4639.

(7) Caseri, W. Inorganic Nanoparticles as Optically Effective Additives for Polymers. *Chem. Eng. Commun.* **2008**, *196*, 549–572.

(8) Corcione, C. E.; Previderio, A.; Frigione, M. Kinetics Characterization of a Novel Photopolymerizable Siloxane-Modified Acrylic Resin. *Thermochim. Acta* **2010**, *509*, 56–61.

(9) Esposito Corcione, C.; Frigione, M. Factors Influencing Photo-Curing Kinetics of Novel UV Cured Siloxane-Modified Acrylic Coatings: Oxygen Inhibition and Composition. *Thermochim. Acta* **2012**, *534*, 21–27.

(10) Corcione, C. E.; Frigione, M. UV-cured Polymer-Boehmite Nanocomposite as Protective Coating for Wood Elements. *Prog. Org. Coat.* **2012**, *74*, 781–787.

(11) Esposito Corcione, C.; Striani, R.; Frigione, M. Hydrophobic Photopolymerizable Nanostructured Hybrid Materials: An Effective Solution for the Protection of Porous Stones. *Polym. Compos.* **2015**, *36*, 1039.

(12) Guo, L.; Jiang, S.; Qiu, T.; Zhang, S.; He, L.; Tan, J.; Li, X. Miniemulsion Polymerization of Fluorinated Siloxane-Acrylate Latex and the Application as Waterborne Textile Finishing Agent. *J. Appl. Polym. Sci.* **2014**, *131*, 40162.

(13) Tighe, B. Contact Lens Materials. In *Contact Lenses*, 5th ed.; Phillips, A. J., Speedwell, L., Eds.; Butterworth-Heinemann: Edinburgh, U.K.; 2006; pp 59–78.

(14) Esposito Corcione, C.; Striani, R.; Frigione, M. UV-Cured Siloxane-Modified Methacrylic System Containing Hydroxyapatite as Potential Protective Coating for Carbonate Stones. *Prog. Org. Coat.* **2013**, *76*, 1236–1242.

(15) Stroyuk, A. L.; Sobran, I. V.; Kuchmiy, S. Y. Photoinitiation of Acrylamide Polymerization by Fe_2O_3 Nanoparticles. *J. Photochem. Photobiol., A* **2007**, *192*, 98–104.

(16) Damm, C. An Acrylate Polymerisation Initiated by Iron Doped Titanium Dioxide. *J. Photochem. Photobiol., A* **2006**, *181*, 297–305.

(17) Stroyuk, A.; Granchak, V. M.; Korzhak, A. V.; Kuchmii, S. Ya. Photoinitiation of Buthylmethacrylate Polymerization by Colloidal Semiconductor Nanoparticles. *J. Photochem. Photobiol., A* **2004**, *162*, 339–351.

(18) Hoffman, A. J.; Mills, G.; Yee, H.; Hoffmann, M. R. Photoinitiated Polymerization of Methyl Methacrylate using Q-sized Zinc Oxide Colloids. *J. Phys. Chem.* **1992**, *96*, 5540–5546.

(19) Shirkavand, S.; Moslehifard, E. Effect of TiO_2 Nanoparticles on Tensile Strength of Dental Acrylic Resins. *J. Dent. Res. Dent. Clin. Dent. Prospects* **2014**, *8*, 197–203.

(20) Chen, C.; Wang, Y.; Pan, G.; Wang, Q. Gel-sol Synthesis of Surface Treated TiO_2 Nanoparticles and Incorporation with Waterborne Acrylic Resin Systems for Clear UV Protective Coatings. *J. Coat. Technol. Res.* **2014**, *11*, 785–791.

(21) Charpentier, P. A.; Burgess, K.; Wang, L.; Chowdhury, R. R.; Lotus, A. F.; Moula, G. Nano-TiO_2/Polyurethane Composites for Antibacterial and Self-Cleaning Coatings. *Nanotechnology* **2012**, *23*, 425606.

(22) Tao, P.; Li, Y.; Rungta, A.; Viswanath, A.; Gao, J.; Benicewicz, B. C.; Siegel, R. W.; Schadler, L. S. TiO_2 Nanocomposites with High Refractive Index and Transparency. *J. Mater. Chem.* **2011**, *21*, 18623–18629.

(23) Cozzoli, P. D.; Kornowski, A.; Weller, H. Low-Temperature Synthesis of Soluble and Processable Organic-Capped Anatase TiO_2 Nanorods. *J. Am. Chem. Soc.* **2003**, *125*, 14539–14548.

(24) Herrmann, J.-M. Heterogeneous Photocatalysis: Fundamentals and Applications to the Removal of Various Types of Aqueous Pollutants. *Catal. Today* **1999**, *53*, 115–129.

(25) Manna, L.; Scher, E. C.; Li, L. S.; Alivisatos, A. P. Epitaxial Growth and Photochemical Annealing of Graded CdS/ZnS Shells on Colloidal CdSe Nanorods. *J. Am. Chem. Soc.* **2002**, *124*, 7136–7145.

(26) De Palma, R.; Peeters, S.; Van Bael, M. J.; Van den Rul, H.; Bonroy, K.; Laureyn, W.; Mullens, J.; Borghs, G.; Maes, G. Silane

DOI: 10.1021/acsami.5b03731
ACS Appl. Mater. Interfaces 2015, 7, 15494–15505

Ligand Exchange to Make Hydrophobic Superparamagnetic Nanoparticles Water-Dispersible. *Chem. Mater.* **2007**, *19*, 1821−1831.
(27) Mirabedini, A.; Mirabedini, S. M.; Babalou, A. A.; Pazokifard, S. Application of Mixture Experimental Design to Optimize Formulation and Performance of Thermoplastic Road Markings. *Prog. Org. Coat.* **2011**, *72*, 453−460.
(28) NORMAL Protocol 33/89, contact angle determinations, icr-cnr, Roma, Italy, 1993; http://www.sbn.it/opacsbn/opaclib?db=solr_iccu=opac/iccu/full.jsp=1=10=opac/iccu/error.jsp=search_show_cmd=none:1032:BID=IT\ICCU\NAP\0275245.
(29) Robinson, D. B.; Persson, H. H.; Zeng, H.; Li, G.; Pourmand, N.; Sun, S.; Wang, S. X. DNA-functionalized MFe_2O_4 (M=Fe, Co, Mn) nanoparticles and their hybridization to DNA-functionalized surfaces. *Langmuir* **2005**, *21*, 3096−3103.
(30) Rostamzadeh, P.; Mirabedini, S. M.; Esfandeh, M. APS-silane modification of silica nanoparticles: effect of treatment's variables on the grafting content and colloidal stability of nanoparticles. *J. Coat. Technol. Res.* **2014**, *11*, 651−660.
(31) Lee, Y.; Guymon, C. A.; Jönsson, E. S.; Hoyle, C. E. The Effect of Monomer Structure on Oxygen Inhibition of (Meth)acrylates Photopolymerization. *Polymer* **2004**, *45*, 6155−6162.
(32) Bongiovanni, R.; Sangermano, M.; Medici, A.; Tonelli, C.; Rizza, G. Nanostructured Hybrid Networks based on Highly Fluorinated Acrylates. *J. Sol-Gel Sci. Technol.* **2009**, *52*, 291−298.
(33) Maffezzoli, A.; Terzi, R. Effect of Irradiation Intensity on the Isothermal Photopolymerization Kinetics of Acrylic Resins for Stereolithography. *Thermochim. Acta* **1998**, *321*, 111−121.
(34) Ni, X.; Ye, J.; Dong, C. Kinetics Studies of Methyl Methacrylate Photopolymerization Initiated by Titanium Dioxide Semiconductor Nanoparticles. *J. Photochem. Photobiol., A* **2006**, *181*, 19−27.
(35) Schmidt, D. L.; Brady, R. F., Jr.; Lam, K.; Schmidt, D. C.; Chaudhury, M. K. Contact Angle Hysteresis, Adhesion, and Marine Biofouling. *Langmuir* **2004**, *20*, 2830−2836.
(36) Lionetto, F.; Mascia, L.; Frigione, M. Evolution of Transient States and Properties of an Epoxy−Silica Hybrid Cured at Ambient Temperature. *Eur. Polym. J.* **2013**, *49*, 1298−1313.

DOI: 10.1021/acsami.5b03731
ACS Appl. Mater. Interfaces 2015, 7, 15494−15505